

RECENT ADVANCES IN HIGH RESOLUTION SAR INTERFEROMETRIC STACKING TECHNIQUES EXPLOITING DISTRIBUTED SCATTERERS

Kanika Goel and Nico Adam

Remote Sensing Technology Institute (IMF), German Aerospace Center (DLR), Germany

ABSTRACT

This paper presents advanced stacking techniques in high resolution SAR interferometry which focus on Distributed Scatterers (DSs). These recently developed algorithms are among the first to exploit meter-resolution spaceborne SAR data and have been applied on test cases which are challenging for conventional multitemporal techniques.

Index Terms— Distributed Scatterer (DS), Deformation Monitoring, Digital Elevation Model (DEM), Interferometric Synthetic Aperture Radar (InSAR), TanDEM-X, TerraSAR-X.

1. INTRODUCTION

Interferometric Synthetic Aperture Radar (InSAR) is a satellite remote sensing technique that provides information about topography and deformation of the Earth's surface [1]. Monitoring of surface deformation is crucial for studying, understanding and forecasting geodynamical processes occurring in mines, reservoirs, landslides, volcanoes and earthquakes. However, InSAR has limitations due to low temporal sampling rate, atmospheric effects and decorrelation (temporal and geometric).

In recent years, InSAR's capabilities have been considerably improved with the launch of high resolution SAR sensors such as TerraSAR-X, TanDEM-X and COSMO-SkyMed. Mapping of urban areas and even single buildings is now facilitated via multitemporal InSAR techniques, for instance, Persistent Scatterer Interferometry (PSI) [2] and SAR Tomography (TomoSAR) [3]. These methods exploit long time coherent Persistent Scatterers (PSs) and provide elevation and surface displacement measurements with a high precision.

However, the density of PSs is low in non-urban areas. It is imperative to fully utilize the potential of high resolution SAR data and increase the spatial density of measured points by utilizing, in addition to the PSs, the partially coherent DSs. Various techniques, for example, the Small Baseline Subset Algorithm (SBAS) [4] and SqueeSAR [5], have been proposed to extract information from DSs. But SBAS is prone to phase unwrapping errors in rural areas and estimates deformation at low resolution, whereas SqueeSAR can be computationally expensive as it processes all possible interferogram combinations.

With respect to the above-mentioned techniques, new/alternative multitemporal approaches for high resolution deformation estimation have been developed which exploit DSs [6]–[8]. With higher resolution, shorter repeat cycles, smaller orbital tubes and higher bandwidth of the satellites; Distributed Scatterer Interferometry (DSI) is now supported by a practical data basis. Additionally, the TerraSAR-X/TanDEM-X mission facilitates bistatic single-pass interferometry. Addition of a few TanDEM-X data pairs (that are free from displacement, atmosphere and temporal decorrelation) to the existing monostatic repeat-pass TerraSAR-X data stack improves the results of stacking techniques in dense metropolitan areas, where spatial phase unwrapping is a challenge due to geometrical limitations such as radar layover and shadow.

This paper describes the newly developed techniques and application test cases using high resolution TerraSAR-X/TanDEM-X data. These techniques provide spatially dense deformation maps for areas characterized either by high temporal decorrelation or by layover problems, and counteract some of the limitations of conventional coherent SAR techniques.

2. METHODOLOGIES AND EXPERIMENTAL RESULTS

The novel techniques and application test cases using TerraSAR-X/TanDEM-X data are presented below.

2.1 An Advanced SBAS Algorithm

An advanced SBAS approach has been developed for high resolution deformation monitoring with a focus on natural terrains characterized by typical temporal decorrelation and phase ambiguities [6]. It is based on an object-adaptive parameter estimation, exploiting only the small baseline differential interferograms so as to reduce the effects of topography on the DSs.

The implementation starts with an adaptive spatial phase filtering algorithm. It reduces the phase noise while maintaining the high geometric resolution provided by new satellites such as TerraSAR-X (meter resolution). Using a stack of coregistered and calibrated SAR amplitude images, the statistically homogenous pixels surrounding each pixel are identified via a statistical test e.g. Anderson-Darling test. The

homogenous pixels identified are then used for pixel-wise adaptive phase flattening of single-look small baseline differential interferograms to compensate for topographic residuals. Here, a periodogram approach is utilized to estimate and remove local gradients of residual DEM in range and azimuth directions. Later, an adaptive complex multi-looking of the flattened interferometric phase of the adaptive neighborhood is performed for an accurate phase and coherence estimation for each pixel.

Subsequently, the phase estimates are used to retrieve the non-linear deformation time series using an L1-norm based SBAS technique. A generic L_p -norm solution is given by:

$$\hat{v} = \arg \min_v \left(\sum_{i=0}^{M-1} |\phi'_{DInSAR} - Bv|_i^p \right)^{\frac{1}{p}} \quad (1)$$

where ϕ'_{DInSAR} is the vector of unwrapped differential interferometric phase values, B is the matrix defining the small baseline combinations used and v is the vector of unknown mean phase velocities between time-adjacent acquisitions. The L2-norm inversion is optimal when Gaussian noise is present in the data. But if L2-norm minimization is used in the presence of a spike, the estimated fit tends to deviate towards the outlier thereby resulting in a wrong estimation. An L1-norm inversion results in a more robust solution with respect to the often-occurring and difficult-to-detect phase unwrapping errors (spike noise) found in non-urban areas.

This algorithm has been used to process the area of Lueneburg in Germany. For deformation mapping using the proposed technique, 17 TerraSAR-X High Resolution Spotlight mode images of the test site from 2010-2011 have been used. Lueneburg is situated in the German state of Lower Saxony. Due to constant salt mining dating back to the 19th century and continuing till 1980, various areas of the town experienced a gradual or high subsidence, became unstable and had to be demolished. The sinking still continues even today. Many ground stations have been established since 1946 to monitor the deformation, but due to the changing subsidence patterns and locations, spaceborne differential SAR interferometric technique has been applied for deformation mapping of Lueneburg. Since October 2010, TerraSAR-X data have been ordered to monitor the subsidence at high resolution. For the non-linear deformation monitoring, 89 small baseline differential interferograms have been generated based on a maximum spatial baseline of 150 m and a maximum temporal baseline of 150 days. DLR's PSI-GENESIS processor has been employed for DInSAR processing. Pixels that have an average coherence of at least 0.3 are used. Deformation estimates for Lueneburg are shown in Fig. 1. The standard deviation of the deformation estimates is between 0 and 3.7 mm.

It is to be noted that there are still many points which are decorrelated and have not been estimated and these might be undergoing deformation as well. New algorithms are required

for measuring such difficult areas characterized by high temporal decorrelation and for providing spatially dense deformation maps. This is the basis for the new model-based technique developed and presented in the next sub-section.

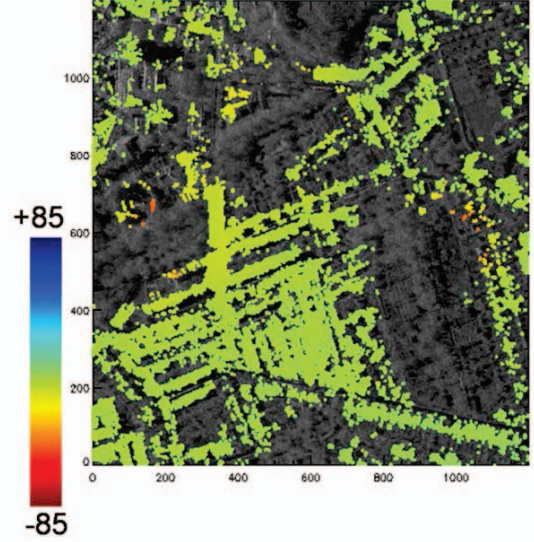


Fig. 1. Deformation velocity in mm/yr estimated for Lueneburg, Germany, via advanced SBAS algorithm exploiting TerraSAR-X data from 2010-2011.

2.2 An Advanced DSI Algorithm

An alternative DSI method has been developed and implemented for deformation velocity monitoring in difficult decorrelated regions whose deformation velocity can be described by a suitable model, exploiting high resolution SAR data [7]. Typical application examples include sub-surface mining areas, sub-surface construction sites and oil/gas/water reservoirs. The proposed method utilizes DSs and consists of three main steps.

First, an identification of DSs, i.e. homogenous object patches of pixels, is done by a similarity test algorithm using a stack of SAR amplitude images as described in the previous sub-section. Then, a robust object-adaptive parameter estimation via a periodogram is performed to estimate the local gradients of deformation velocity and the local gradients of residual DEM in range and azimuth directions for these patches, utilizing small baseline differential interferograms. Finally, since the independent estimated neighboring patches are close and deformation is assumed to be smooth, a 2D model-based deformation integration is performed to get the LOS deformation velocity. To implement this inversion, a Bayesian estimation framework is applied which makes use of directed graphs and particle filters.

The new concept with respect to the existing DS algorithms is that there is no need for conventional spatial phase unwrapping (based on estimation of phase gradients, followed by their integration) and the mean deformation velocity is estimated at a suitable resolution in the order of the dimension of objects. The computational complexity is reduced, as

compared to SqueeSAR, by making use of only small baseline differential interferograms. Even in the presence of high phase noise, the algorithm compensates DEM errors and atmospheric artifacts. Due to model-based deformation integration, a spatially dense deformation velocity map is estimated, instead of just a few measured points.

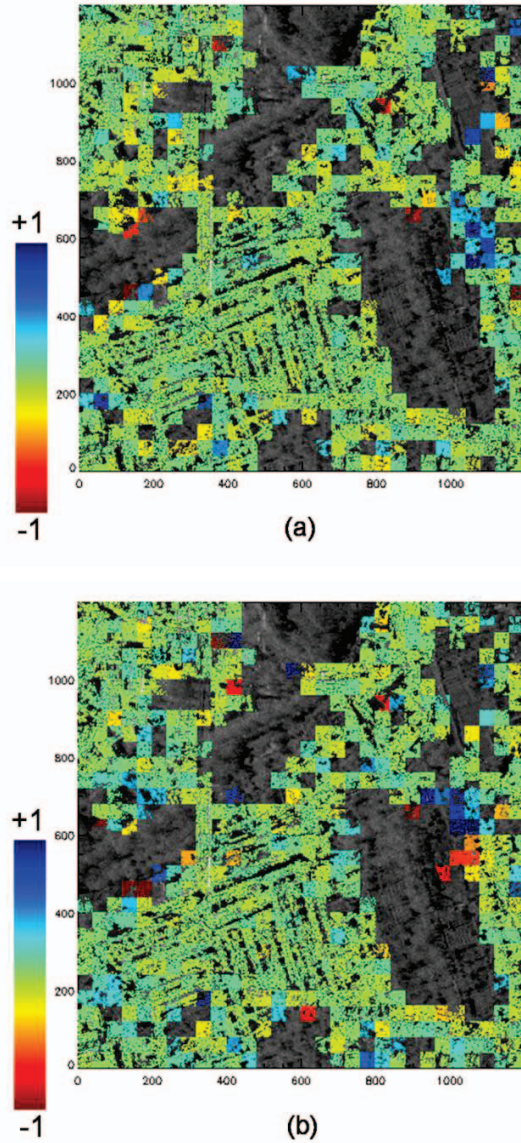


Fig. 2. Deformation gradient estimation results for Lueneburg, Germany, using 89 small baseline differential interferograms. (a) Local gradients of deformation velocity in range (x) direction in mm/year/pixel. (b) Local gradients of deformation velocity in azimuth (y) direction in mm/year/pixel.

The practical demonstration of this technique is provided using TerraSAR-X data of Lueneburg (described in the previous sub-section). The region was divided into rectangular blocks of 40 pixels by 40 pixels, i.e. 24 m by 24 m approximately. Within each block, homogenous pixels were identified by means of the Anderson-Darling statistical test

based on a minimum patch size of 400 pixels and a coherence threshold of 0.3. Fig. 2 visualizes the gradient estimation results for the deformation velocity in range and azimuth directions in mm/year/pixel. The gradients have been estimated for a total of 536,456 points in an area of 1200 pixels by 1200 pixels. The high density of information which can be extracted using the DSI technique can be seen by comparing Fig. 2 with Fig. 1 (which has only 121,024 estimated points). The deformation integration results using the DSI technique are presented in Fig. 3. Gaussian elliptical subsidence has been assumed for the test site, which has undergone salt mining induced subsidence. This is because the most common shape of surface deformation due to mining is a circular or elliptical sag. The results obtained for Lueneburg show two Gaussian subsidence bowls, one having a larger deformation than the other and also covering a larger area. The features which have been identified as deforming in Fig. 1 are also deforming in Fig. 3.

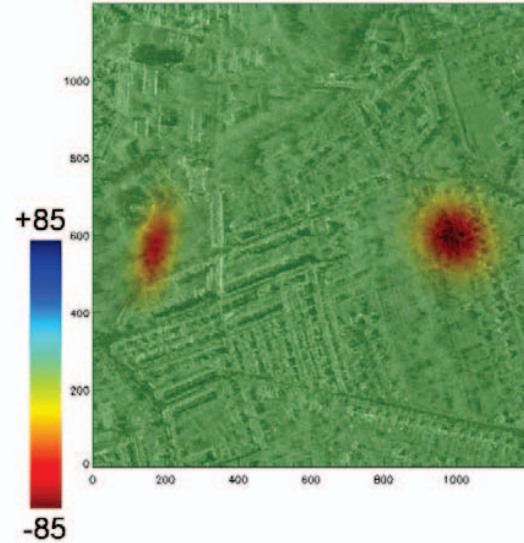


Fig. 3. Deformation velocity in mm/year estimated for Lueneburg, Germany, via advanced DSI algorithm exploiting TerraSAR-X data from 2010-2011.

2.3 Fusion of Monostatic and Bistatic InSAR Stacks for DSs

A fusion technique is demonstrated to jointly process monostatic and bistatic TerraSAR-X/TanDEM-X InSAR stacks exploiting DSs for complex urban area monitoring and by-passing scattering scenarios, for instance, radar layover [8].

The bistatic and monostatic (small baseline) interferograms are first spatially adaptive multi-looked and DSs are selected. The bistatic interferograms with no deformation and atmospheric phase components are then exploited for topography estimation of each DS (no external DEM is used). Given M spatially adaptive multi-looked bistatic interferograms with different perpendicular baselines (and thus, different height of ambiguities) and referenced with

respect to a single pixel, it is possible to retrieve the height h for each DS by using its wrapped interferometric phase vector. The height of a DS here refers to the average height of the DS area which has been multi-looked. Since a pixelwise adaptive multi-looking has been performed, areas with sloping or complex topography are appropriately handled. The following model coherence function (periodogram) ξ is maximized for height estimation:

$$\xi(h) = \frac{1}{M} \left| \sum_{k=1}^M e^{j(\phi_{obs}^k - \phi_{model}^k)} \right|, \phi_{model}^k = \frac{2\pi}{\lambda} \frac{B_{\perp}^k}{R \sin \theta} h \quad (2)$$

where ϕ_{obs}^k and ϕ_{model}^k are the observed (spatially adaptive multi-looked) and modeled interferometric phases, respectively, for a generic pixel in the k th bistatic interferogram with baseline B_{\perp}^k , λ is the signal wavelength, R is the range distance determined by precisely measuring the time from transmission of a pulse to receiving the echo from the target and θ is the look angle. Since there is no deformation phase in the bistatic interferograms, the periodogram is a 1D function dependent just on the DS's height (and not on its velocity) and its values are known over an irregular grid defined by the available spatial baselines. The topography estimate for each DS is estimated from the peak of this periodogram, i.e.:

$$(\hat{h}) = \arg \max_h (\xi) \quad (3)$$

The maximum of the periodogram is the temporal coherence of the DS. The precision of the estimation depends on the number of bistatic interferograms, their baseline distribution, phase stability of the DS and the sensor characteristics. The estimated topographic phases are subsequently removed from the monostatic interferograms and the L1-norm based SBAS technique is applied to retrieve the residual topography and deformation time series of each DS.

An illustration of this fusion algorithm is provided using 84 'High Resolution Spotlight' TerraSAR-X/TanDEM-X images of Las Vegas, US, from 2008-2011. 5 bistatic interferograms and 174 small baseline monostatic differential interferograms were generated. Fig. 4 shows the elevation and root-mean-square (RMS) deformation estimates.

3. CONCLUSION

The multitemporal techniques and applications presented in this paper broaden the scope of SAR interferometry for deformation and topographic mapping in difficult areas by exploiting high resolution SAR data. These developed estimation principles improve the robustness and precision of deformation estimates for DSs.

REFERENCES

- [1] R. Bamler and P. Hartl, "Synthetic aperture radar interferometry- Topical review," Inverse problems- 14, R1 - R54, IOP Publishing Limited (UK), 1998.
- [2] A. Ferretti, C. Prati, and F. Rocca, "Permanent scatterers in SAR interferometry," IEEE TGARS, vol. 39, no. 1, pp. 8-20, 2001.
- [3] X. Zhu and R. Bamler, "Very high resolution spaceborne SAR tomography in urban environment," IEEE TGARS, vol. 48, no. 12, pp. 4296-4308, 2010.
- [4] P. Berardino, G. Fornaro, R. Lanari, and E. Sansosti, "A new algorithm for surface deformation monitoring based on small baseline differential SAR interferograms," IEEE TGARS, vol. 40, no. 11, pp. 2375-2383, 2002.
- [5] A. Ferretti, A. Fumagalli, F. Novali, C. Prati, F. Rocca, and A. Rucci, "A New Algorithm for processing interferometric data-stacks: SqueeSAR," IEEE TGARS, vol. 49, no. 9, pp. 3460-3470, 2011.
- [6] K. Goel and N. Adam, "An advanced algorithm for deformation estimation in non-urban areas," ISPRS Journal of Photogrammetry and Remote Sensing, vol. 73, pp. 100-110, 2012.
- [7] K. Goel and N. Adam, "A distributed scatterer interferometry approach for precision monitoring of known surface deformation phenomena," IEEE TGARS, vol. PP, no. 99, pp. 1-15, doi: 10.1109/TGRS.2013.2289370, 2013.
- [8] K. Goel and N. Adam, "Fusion of monostatic/bistatic InSAR stacks for urban area analysis via distributed scatterers," IEEE GRSL, vol. 11, no. 4, pp. 733-737, April 2014.

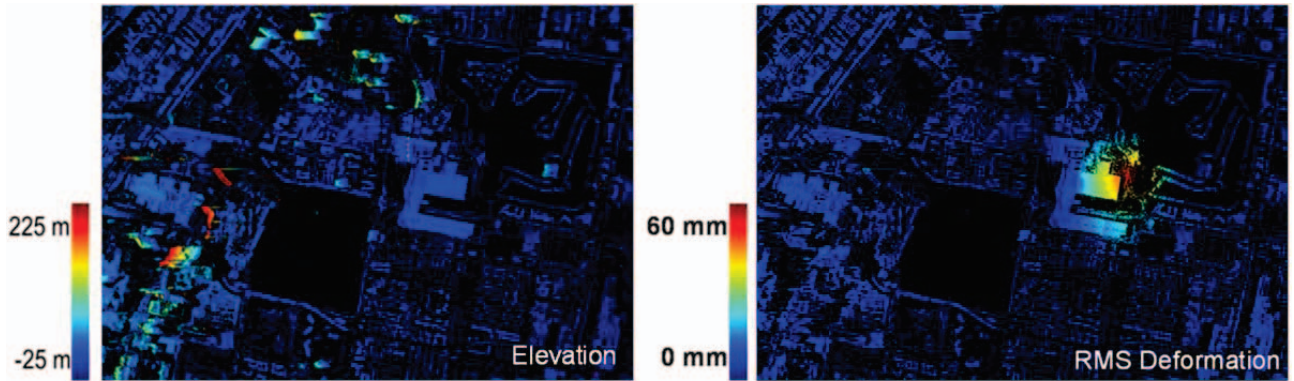


Fig. 4. Elevation and root-mean-square (RMS) deformation estimates for Las Vegas, US, exploiting TerraSAR-X/TanDEM-X data from 2008-2011.